ChemComm

COMMUNICATION

View Article Online
View Journal | View Issue

Cite this: *Chem. Commun.*, 2016, 52, 13471

Received 6th July 2016,
Accepted 23rd October 2016

DOI: 10.1039/c6cc05576a

www.rsc.org/chemcomm

Rapid characterization of folding and binding interactions with thermolabile ligands by DSC†

R. W. Harkness V,[a] S. Slavkovic,[b] P. E. Johnson[b] and A. K. Mittermaier*[a]

Differential scanning calorimetry (DSC) is a powerful technique for measuring tight biomolecular interactions. However, many pharmaceutically relevant ligands are chemically unstable at the high temperatures used in DSC analyses. Thus, measuring binding interactions is challenging because the concentrations of ligands and thermally-converted products are constantly changing within the calorimeter cell. Using experimental data for two DNA aptamers that bind to the thermolabile ligand cocaine, we present a new global fitting analysis that yields the complete set of folding and binding parameters for the initial and final forms of the ligand from a pair of DSC experiments, while accounting for the thermal conversion. Furthermore, we show that the rate constant for thermolabile ligand conversion may be obtained with only one additional DSC dataset.

Characterizing binding interactions between biomolecules and pharmaceutical compounds is critical for guiding the drug design process.[1–5] Calorimetry is a powerful approach for measuring such interactions because it directly detects the heat evolved from binding with no sample labelling required (*e.g.* fluorescent tags). In particular, differential scanning calorimetry (DSC) allows the characterization of ultra-tight binding interactions in addition to biomolecular denaturation profiles.[6,7] Ligand binding is detected as an upshift in the thermal denaturation temperature as the bound state is stabilized. Though ligand interaction studies by DSC are relatively straightforward to implement, the repeated scanning to high temperatures can be problematic. For example, many important pharmaceutical compounds undergo rearrangement or decomposition when exposed to high temperatures,[8–13] *i.e.* they are thermolabile. DSC analyses typically involve running multiple cycles of heating and cooling on the same sample, and good reproducibility of the scans is considered a prerequisite for thermodynamic analyses.[14] Thermal conversion of a ligand to a secondary form with altered binding characteristics can lead to pronounced differences between replicate thermograms, since the concentration of the original ligand decreases with each scan while thermal conversion products accumulate. These data sets are not interpretable in traditional DSC analyses.

Here we show that, in fact, data sets for thermolabile ligands are information rich. We have examined the folding and binding interactions of two cocaine-binding DNA aptamers, MN4 and MN19 with the thermolabile ligand cocaine (Fig. 1). The aptamers are also capable of binding quinine, and, because quinine does not readily convert to a secondary ligand within the DSC temperatures used here, we employed quinine as a negative control for thermal conversion. MN4 contains three complete stems and is folded in its free state, while MN19 has a truncated stem 1 and is largely unstructured when not bound to ligand.[15] We have developed a global analysis that simultaneously yields the parameters of biomolecular folding and binding for the initial and thermal product ligand. Global analysis of the thermogram series permits the extraction of both folding and binding thermodynamics from just two DSC experiments performed in the presence and absence of a thermolabile ligand. This represents significant savings in time

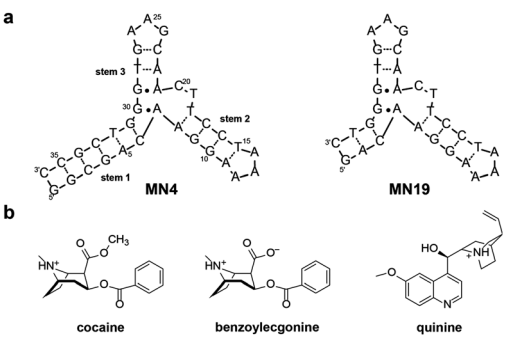

Fig. 1 Cocaine binding aptamers, thermolabile ligand, thermal conversion product, and thermostable control. (a) Aptamers with base pair hydrogen bonds shown as dashed lines. (b) Chemical structures of ligands investigated by DSC.

[a] *Department of Chemistry, McGill University, 801 Sherbrooke St. W., Montreal QC H3A 0B8, Canada. E-mail: anthony.mittermaier@mcgill.ca*
[b] *Department of Chemistry, York University, 4700 Keele Street, Toronto ON M3J 1P3, Canada*

† Electronic supplementary information (ESI) available. See DOI: 10.1039/c6cc05576a

and material compared to non-heat-labile ligands, as multiple (~7–10) separate DSC experiments must typically be set up to obtain a similar set of data.[6] In addition, we show that the rate constant for ligand thermal conversion may be calculated with as little as one additional experiment.

Thermolabile ligands gradually convert from an initial to a secondary form when exposed to elevated temperatures. For example, cocaine spontaneously converts to benzoylecgonine[16] at higher temperatures (70–80 °C). We exploited this property in characterizing the interactions of MN4 and MN19 with cocaine by DSC (Fig. 2).

In a previous investigation we found by ITC that MN4 and MN19 have moderate affinities for cocaine (K_D = 7 and 27 μM respectively), and MN4 has undetectable affinity for benzoylecgonine.[15,18]

The aptamers have stronger affinities for quinine (K_D = 0.23 and 0.70 μM for MN4 and MN19 respectively).[19] The series of replicate DSC thermograms obtained for MN4 and MN19 with cocaine are shown in Fig. 2a and b. Each successive DSC denaturation profile shifts towards lower temperatures and smaller heights. We attribute this to the progressive conversion of cocaine to the more weakly binding benzoylecgonine. After a large number of scans (roughly 7–10), the apparent melting temperature stabilizes at a new lower value, which we interpret as 100% conversion of cocaine to benzoylecgonine. These asymptotic scans indicate that both MN4 and MN19 bind benzoylecgonine; in the case of MN4, a slight thermal upshift and increase in peak height is apparent compared to the thermogram of the free aptamer (Fig. S1a and S2, ESI†). In the case of MN19, the asymptotic scans exhibit clear unfolding peaks, while an almost non-existent unfolding peak was observed for the free MN19 molecule (Fig. S2c, ESI†). Notably, repeat scans for both aptamers in the presence of the thermostable quinine ligand are superimposable (Fig. 2c, d and Fig. S1b, d, ESI†).

We have developed a global analysis method for DSC data obtained with thermolabile ligands that yields folding and binding parameters for the initial and thermally converted ligand from a pair of experiments performed with and without added ligand. This represents considerable savings in material and experiment time, as DSC-based ligand binding assays typically involve repeating multiple (~7–10) experiments over a range of ligand concentrations.[6]

The analysis (see ESI,† Methods for details) yielded the enthalpy, ΔH, and entropy, ΔS, of the folding, cocaine-binding, and benzoylecgonine-binding reactions (Table 1), as well as the extent of ligand thermal conversion in each scan (Table S1, ESI†). The folding thermodynamic parameters obtained for MN4 with both cocaine and quinine are equal within experimental uncertainties, as expected since the stability of the free biomolecule should not depend on the identity of dilute co-solutes. The global binding parameters for both aptamers with cocaine and quinine (Table 1, B1F parameters) are in good agreement with isothermal titration calorimetry (ITC)-derived parameters,[15,18,19] despite differences in buffer, providing proof-of principle for this method. Interestingly, the DSC parameters show that the preference of MN4 for quinine over cocaine is driven by a much more favourable binding enthalpy. Conversely, the preference of

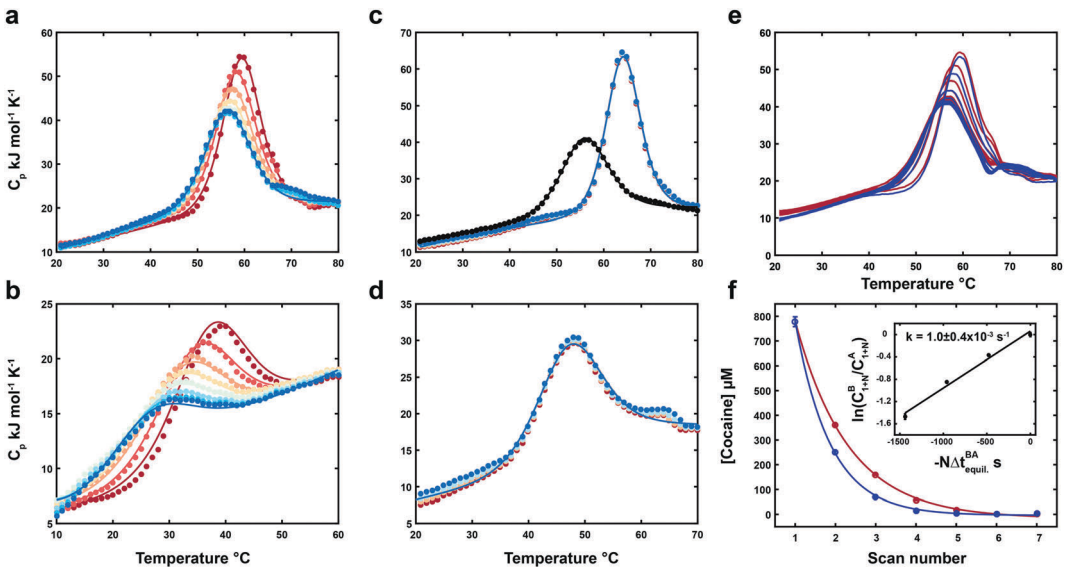

Fig. 2 Rapid characterization of folding and binding thermodynamics using thermolabile ligands. (a) DSC heat capacity profiles for MN4 bound to cocaine and benzoylecgonine. (b) DSC heat capacity profiles for MN19 bound to cocaine and benzoylecgonine. (c) DSC heat capacity profiles for MN4 both free and bound to quinine. (d) DSC heat capacity profiles for MN19 bound to quinine. Ligand-bound experimental data points are shown as colored filled circles, fits are shown as colored lines. The first and last scans are red and blue respectively. Experimental and fitted data for free MN4 are shown as black circles and lines respectively. (e) Sets of DSC profiles for MN4 bound to cocaine and benzoylecgonine. The red profiles have equilibration times of 120 seconds at 80 °C between scans, the blue profiles have 600 second equilibration times between scans. (f) The cocaine concentrations from global analysis of datasets in (e) as a function of scan number. Experimental points and fits are shown as colored empty circles and lines respectively. Exponential fits were performed according to [cocaine] = a + [cocaine]$_0$ exp$^{(-b*\text{scan number})}$. The inset shows a linear fit to ESI,† eqn (S19) for the first 4 forward scans of the 120 (A) and 600 second (B) equilibration time datasets.

Table 1 Thermodynamic parameters extracted from global analysis of DSC data using thermolabile and thermostable ligands

	MN4		[b]MN19	
Fit parameters	Cocaine added	Quinine added	Cocaine added	Quinine added
ΔH^{UF}	271.3 ± 1.8	272.5 ± 4.0	—	—
ΔS^{UF}	824.4 ± 5.1	827.9 ± 10.9	—	—
ΔG^{UF}[a]	21.6 ± 0.2	21.6 ± 0.9	—	—
ΔH^{B1F}[a]	−75.2 ± 1.6	−101.0 ± 4.0	−148.1 ± 1.4	−105.9 ± 10.4
ΔS^{B1F}[a]	−154.2 ± 5.0	−213.7 ± 12.0	−418.2 ± 7.9	−264.9 ± 34.1
ΔC_p^{B1F}	−1.5 ± 0.1	−1.2 ± 0.1	−5.2 ± 0.1	−7.0 ± 0.3
ΔG^{B1F}[a]	−28.5 ± 0.2	−36.2 ± 0.7	−21.4 ± 0.1	−25.6 ± 0.2
ΔH^{B2F}[a]	−33.7 ± 1.8	—	−155.7 ± 2.4	—
ΔS^{B2F}[a]	−49.9 ± 5.2	—	−469.8 ± 8.0	—
ΔC_p^{B2F}	−2.2 ± 0.1	—	−8.2 ± 0.2	—
ΔG^{B2F}[a]	−18.6 ± 0.3	—	−13.3 ± 0.1	—

[a] Parameters were calculated at 30 °C. [b] MN19 was assumed to be only folded when bound to ligand, the parameters listed here are for unfolding of the bound folded state. B1F refers to cocaine- or quinine-bound folded states and B2F refers to the benzoylecgonine-bound folded state. ΔH and ΔG are expressed in kJ mol^{-1}, ΔS is expressed in J mol^{-1} K^{-1}and ΔC_p is expressed in kJ mol^{-1} K^{-1}. Errors were calculated according to the variance/co-variance method.[17]

MN19 for quinine over cocaine is driven by a much less unfavourable binding entropy term. The analysis also yielded the binding parameters for benzoylecgonine (Table 1, B2F parameters), with K_D = 604 μM and 5.1 mM, for MN4 and MN19 respectively. This demonstrates the sensitivity of DSC in measuring very weak binding interactions, as benzoylecgonine binding to MN4 and similar aptamers was previously undetected by ITC, absorbance, and fluorescence spectroscopy.[18,20,21] Similar to what was observed for quinine, the preference of MN4 for cocaine over benzoylecgonine is due to a more favourable binding enthalpy, while in the case of MN19 it is due to a less unfavourable binding entropy. This points to a common energetic mechanism underlying the selectivity of aptamer binding and highlights the importance of obtaining thermodynamic information for understanding molecular interactions.

As expected, the thermal conversion of cocaine proceeds further with each successive thermogram, following a single exponential decay as a function of scan number (Fig. 2e, f and Table S1, ESI†). In actuality, thermally labile ligands convert to their secondary products continuously throughout each DSC scan, with the rate accelerating as the temperature increases, according to the activation enthalpy.[22] We made the simplifying assumption in the global analysis that the concentration is constant during each scan, but varies scan-to-scan. This assumption depends both on the rate of thermal conversion and the temperature scan rate of the calorimeter. In order to test the effects of these parameters and identify optimal ranges, we performed computer simulations with different ligand conversion kinetics and scan rates in ESI,† Fig. S3 and S4. Importantly, thermograms generated with fixed and varying ligand concentrations at 1 °C min^{-1} scan rate are superimposable (Fig. S3a, ESI†) indicating that the ligand concentration can indeed be treated as constant in each scan. This makes sense as the conversion rate is ∼10 000-fold faster at 80 relative to 0 °C at pH 6.8. The simulations imply that, at least in this case, ligand conversion occurs almost entirely during the high temperature portion of the scans where the thermograms are not dependent on ligand concentration. It must be noted that in cases where ligand conversion is less temperature dependent or when the biomolecular melting temperature is much higher, this assumption might not be expected to hold. We find that when the ratio of the scan rate (°C min^{-1}) to the rate constant for ligand conversion at the apparent T_m of the first forward scan (min^{-1}) is ∼ ≤20 °C, the assumption breaks down. It would in principle be possible to fit DSC data with continuously-varying ligand concentrations (essentially an extension of the simulations above), however this is unnecessary for the data at hand.

When the thermal conversion products bind less tightly than the original ligand, the apparent melting temperatures decrease in successive DSC scans, as observed for MN4 and MN19 interacting with cocaine. In the limit that the thermal conversion product does not bind at all, the unfolding thermogram of the ligand-free biomolecule is eventually obtained after a sufficient number of scans. However, it is not possible to determine from these endpoint scans alone whether the thermal conversion product binds weakly or not at all. For that reason, it is important to jointly analyze the thermogram of the free biomolecule, as a reference. Conversely, if the thermal conversion product binds more tightly than the original ligand, then apparent melting temperatures increase with successive DSC scans, reaching a maximum when full conversion of the ligand is achieved. In order to illustrate possible scenarios (conversion products with no, weaker, and tighter binding) we performed simulations shown in ESI,† Fig. S5.

In addition to the thermodynamic parameters describing the folding and binding processes, the rate constant for thermal conversion is also of interest. This can be obtained in a straightforward manner by performing one additional biomolecule/ligand DSC experiment with a different high-temperature equilibration time. When a longer equilibration time is chosen, the scan-to-scan changes in ligand concentrations are greater, with a concomitant increase in the differences between successive thermograms. The ratios of successive ligand concentrations can be fit to yield the rate constant for conversion at the equilibration temperature (see ESI,† Methods). We performed two sets of MN4/cocaine DSC experiments with either 120- or

600 second equilibration times between repeat scans. The scan-to-scan decrease in ligand concentration is far more pronounced for the 600 second dataset compared to the 120 second dataset (Fig. 2e), as anticipated. Conversion of cocaine to benzoylecgonine follows pseudo-first order kinetics and from the cocaine concentrations extracted from the global fits, we fit ESI,† eqn (S19) to obtain a rate constant for cocaine conversion of $1.0 \pm 0.4 \times 10^{-3}$ s^{-1} (Fig. 2f inset), in close agreement to the value previously determined at 80 °C ($1.7 \pm 0.3 \times 10^{-3}$ s^{-1}, citric acid-phosphate buffer pH 7.65).[16]

Oligonucleotide samples were purchased pre-purified from Integrated DNA Technologies (Iowa, USA). Samples were dissolved in 20 mM sodium phosphate buffer, 140 mM NaCl, pH 7.4. DNA concentrations were 83 and 88 μM for MN4 and MN19. Initial ligand concentrations were 778 and 880 μM for cocaine and quinine respectively.

Each experiment consisted of 10 melting and 10 annealing scans. Scan rates were 1.0 °C min^{-1}. Samples were scanned from 0–80 °C with equilibration times of 60 seconds between scans, except for the cocaine kinetics experiments which used 120 and 600 second equilibration times.

DSC is a powerful approach for characterizing biomolecule/ligand interactions, with many applications in drug development.[1–4] It is particularly well-suited to very tight interactions that are difficult to study directly by titration methods such as ITC.[23,24] We find here that DSC is also highly effective at measuring very weak binding interactions (high μM to mM) that may be undetectable by other techniques. DSC has the additional advantage of simultaneously providing information on both folding and binding reactions. However, the thermal lability of many known pharmaceuticals and potential drug leads can lead to DSC data with large scan-to-scan variations that are not interpretable using standard methods. Our global fitting method exploits these variations to yield folding and binding parameters in a fraction of the time and sample needed for thermally-stable compounds analyzed with conventional DSC approaches. Furthermore, just one additional DSC experiment gives the rate constant for thermal conversion. This method therefore opens the door to using DSC to characterize a class of hitherto inaccessible biomolecule/ligand interactions with high precision.

This research was supported by the Natural Sciences and Engineering Research Council (NSERC, Canada, grant number 327028-09 (A. K. M.) and 238562 (P. E. J.)). R. W. H. V. was supported by the NSERC CREATE Training Program in Bionanomachines.

References

1 G. Bruylants, J. Wouters and C. Michaux, *Curr. Med. Chem.*, 2005, **12**, 2011–2020.
2 N. C. Garbett and J. B. Chaires, *Expert Opin. Drug Discovery*, 2012, **7**, 299–314.
3 G. A. Holdgate and W. H. J. Ward, *Drug Discovery Today*, 2005, **10**, 1543–1550.
4 V. Plotnikov, A. Rochalski, M. Brandts, J. F. Brandts, S. Williston, V. Frasca and L. N. Lin, *Assay Drug Dev. Technol.*, 2002, **1**, 83–90.
5 A. Schon, S. Y. Lam and E. Freire, *Future Med. Chem.*, 2011, **3**, 1129–1137.
6 J. F. Brandts and L. N. Lin, *Biochemistry*, 1990, **29**, 6927–6940.
7 P. L. Privalov and A. I. Dragan, *Biophys. Chem.*, 2007, **126**, 16–24.
8 M. M. I. Ali Kamal Attia and M. Abdel Nabi El-Ries, *Adv. Pharm. Bull.*, 2013, **3**, 419–424.
9 B. J. Berendsen, I. J. Elbers and A. A. Stolker, *Food Addit. Contam., Part A: Chem., Anal., Control, Exposure Risk Assess.*, 2011, **28**, 1657–1666.
10 P. Czarniak, M. Boddy, B. Sunderland and J. D. Hughes, *Drug Des., Dev. Ther.*, 2016, **10**, 1029–1034.
11 G. L. A. Kenneth, A. Connors, V. J. Stella, *Chemical Stability of Pharmaceuticals: A Handbook for Pharmacists*, Wiley-Interscience, U. S. A., 1986.
12 A. G.-L. L. Periánez Parraga, I. Gamón Runnenberg, R. Seco Melantuche, O. Delgado Sánchez and F. Puigventós Latorre, *Farm. Hosp.*, 2011, **35**, 1–28.
13 C. L. S. M. K. Hsieh, J. W. Liao, C. A. Franje, Y. J. Huang, S. K. Chang, P. Y. Shih and C. C. Chou, *Vet. Med.*, 2011, **56**, 274–285.
14 J. L. Mergny and L. Lacroix, *Oligonucleotides*, 2003, **13**, 515–537.
15 M. A. Neves, O. Reinstein and P. E. Johnson, *Biochemistry*, 2010, **49**, 8478–8487.
16 J. B. Murray and H. I. Alshora, *J. Clin. Pharm.*, 1978, **3**, 1–6.
17 J. Tellinghuisen, *J. Phys. Chem. A*, 2001, **105**, 3917–3921.
18 S. Slavkovic, M. Altunisik, O. Reinstein and P. E. Johnson, *Bioorg. Med. Chem.*, 2015, **23**, 2593–2597.
19 O. Reinstein, M. Yoo, C. Han, T. Palmo, S. A. Beckham, M. C. Wilce and P. E. Johnson, *Biochemistry*, 2013, **52**, 8652–8662.
20 M. N. Stojanovic, P. de Prada and D. W. Landry, *J. Am. Chem. Soc.*, 2000, **122**, 11547–11548.
21 M. N. Stojanovic and D. W. Landry, *J. Am. Chem. Soc.*, 2002, **124**, 9678–9679.
22 J. d. P. Peter Atkins, *Atkins' Physical Chemistry*, Oxford University Press, Great Britain, 8th edn, 2006.
23 T. Wiseman, S. Williston, J. F. Brandts and L. N. Lin, *Anal. Biochem.*, 1989, **179**, 131–137.
24 A. Velazquez-Campoy and E. Freire, *Nat. Protoc.*, 2006, **1**, 186–191.

